Neurotoxicology 71 (2019) 102–112

Contents lists available at ScienceDirect

Neurotoxicology

journal homepage: www.elsevier.com/locate/neuro

Full Length Article

Involvement of β-catenin in cytoskeleton disruption following adult neural stem cell exposure to low-level silver nanoparticles

Robert J. Cooper, Maya N. Menking-Colby, Kenneth A. Humphrey, Jack H. Victory, Daniel W. Kipps, Nadja Spitzer*

Department of Biological Sciences, Marshall University, One John Marshall Dr., Huntington, WV, 25755, United States

ARTICLE INFO

Keywords:
Time lapse microscopy
f-actin
Neurogenesis
Differentiation
Emerging environmental contaminant

ABSTRACT

Silver nanoparticles (AgNPs) are increasingly incorporated in consumer products to confer antibacterial properties. AgNPs are shed during everyday use of these products, resulting in ingestion or inhalation and bioaccumulation in tissues including the brain. While these low levels of AgNPs do not induce DNA fragmentation typical of apoptosis or necrosis, they do interfere with cytoskeletal structure and dynamics in cultured differentiating adult neural stem cells (NSCs). Moreover, these cells form f-actin inclusions in response to 1 μg/ml AgNPs. Here, we report that these cytoskeletal inclusions colocalize with aggregates of the signaling protein β-catenin, a modulator of cytoskeletal dynamics. Pharmacological alteration of β-catenin signaling reduced formation of f-actin inclusions. AgNP exposure also resulted in a reduction of neurite length in differentiating NSCs, which was mimicked by pharmacological activation of β-catenin signaling. Conversely, pharmacological inhibition of the Wnt/β-catenin signaling pathway resulted in increased neurite lengths in control cells, but did not reverse the neurite collapse induced by AgNP exposure. Substantial changes in neurite length, in response to low-level AgNP or pharmacological manipulation of β-catenin signaling, occurred within the first six hours of exposure and were most evident in cells differentiating towards neural-like morphologies. We conclude that low-level exposure to AgNP, such as that resulting from use of consumer products, may disrupt β-catenin signaling in neural cells in an indirect or non-additive manner. Exposure to AgNP shed from consumer products at levels currently considered safe, may therefore alter physiological function of neural cells. This is of concern particularly regarding children, whose brains contain many developing neurons, and who may face bioaccumulation of AgNP over decades of exposure.

1. Introduction

Silver nanoparticles (AgNPs) are engineered structures with at least one dimension between 1–100 nm. They have novel properties distinct from elemental, ionic, or colloidal silver (Garcia-Reyero et al., 2014; Ivask et al., 2014; Tang et al., 2008; Xiu et al., 2011), and are powerful antimicrobials (Panacek et al., 2006; Samuel and Guggenbichler, 2004; Sondi and Salopek-Sondi, 2004). For this reason, AgNPs are used in manufacturing of consumer products including textiles, plastics, and appliances, which then shed low levels of AgNPs into the environment during use. These can be inhaled or ingested, leading to chronic low-level exposure that is not yet well understood in terms of dosage or risk. (Addo Ntim et al., 2018; Bidgoli et al., 2013; Cushen et al., 2014; Echegoyen and Nerin, 2013; Jokar et al., 2017; Quadros et al., 2013; von Goetz et al., 2013). However, animal studies indicate that internalized AgNPs bypass barrier tissues and membranes, accumulating and persisting in organs including the brain (Lee et al., 2013; Tang et al., 2008; Tang et al., 2010), and leading to chronic low levels of AgNPs in tissues. Though the toxicity of high AgNP concentrations on mammalian cells is well documented (Bartlomiejczyk et al., 2013; Kruszewski et al., 2011), the effects of these low-level exposures are not as well understood.

Neural stem cells (NSCs) occupy several distinct niches in adult brains including the subventricular zone (SVZ), which has been extensively characterized (Altman and Das, 1965; Eriksson et al., 1998; Gage, 2000). Throughout life, NSC from the SVZ (SVZ-NSC) proliferate, giving rise to rapidly dividing migratory precursor cells, and differentiating into neurons and glia (Aimone et al., 2014). This process, adult neurogenesis, is involved in basic functions like learning, memory, and repair (Snyder et al., 2001; van Praag et al., 1999). Proliferating undifferentiated SVZ-NSC isolated from adult rats can be maintained as neurospheres, and induced to differentiate, *in vitro*

* Corresponding author.
E-mail address: spitzern@marshall.edu (N. Spitzer).

https://doi.org/10.1016/j.neuro.2018.12.010
Received 11 October 2018; Received in revised form 30 November 2018; Accepted 28 December 2018
Available online 31 December 2018
0161-813X/ © 2019 Elsevier B.V. All rights reserved.

(Doetsch et al., 2002; Reynolds and Weiss, 1992; Wachs et al., 2003). These cultures offer a robust model for investigating changes to neurodevelopment, developing brain cells, and neural cells following exposure to toxins (Cooper and Spitzer, 2015; Ge et al., 2008).

Previously, we found that low-level (1 μg/mL) AgNPs alter cytoskeleton dynamics in cultured differentiating SVZ-NSC, indicated by formation of f-actin inclusions and disruption of neurite extension dynamics and arborization (Cooper and Spitzer, 2015). Here, we explore the involvement of β-catenin signaling, the canonical endpoint of Wnt pathway, in mediating AgNP effects on cytoskeletal processes (Jamieson et al., 2012). We also used an established model of neurite extension and cell migration, B35 neuroblastoma cells, to investigate changes in β-catenin levels after AgNP exposure. Normally, activation of Wnt signaling leads to accumulation of β-catenin, causing its translocation into the nucleus to bind transcription factors (Xiu et al., 2011). In SVZ-NSC, tightly controlled β-catenin signaling is responsible for maintenance of cell proliferation and induction of differentiation (Adachi et al., 2007; Marinaro et al., 2012; Toledo et al., 2008; Varela-Nallar and Inestrosa, 2013; Wisniewska, 2013). This signaling pathway also plays a role in regulation of neurite extension (Lee et al., 2014), identifying it as a potential target of AgNPs. Disruption of Wnt/β-catenin signaling by AgNPs could lead to deficits in adult neurogenesis, and therefore impairment of basic functions like learning and memory.

2. Methods

2.1. Cell culture

SVZ-NSC were isolated from female young adult (2–6 months old) Sprague-Dawley rats (Hilltop Lab Animals, Scottsdale, PA) and maintained as free-floating neurospheres in the presence of epidermal growth factor (EGF) and fibroblast growth factor - basic (bFGF) (both from Thermo Fisher, Waltham, MA) as previously described (Cooper and Spitzer, 2015), following established protocols (Muraoka et al., 2008; Reynolds and Weiss, 1992; Wachs et al., 2003). SVZ-NSC neurosphere cultures from each animal were kept separate and are considered independent cell lines. Neurospheres were passaged by dissociation with accutase (Thermo Fisher) before reaching a diameter greater than 500 μm (7–14 days) and gave rise to new neurospheres. All protocols were approved by the Marshall University Institutional Animal Care and Use Committee.

For experimentation, undifferentiated neurospheres (passage 4–18) were collected by centrifugation, washed with phosphate-buffered saline 1 (PBS1, in mM: NaH_2PO_4, 2.69 (Sigma, St. Louis, MO); Na_2HPO_4, 11.9 (AMRESCO, Solon, OH); NaCl, 137 (Thermo Fisher, Waltham, MA); KCl, 27 (AMRESCO); pH 7.4), and plated onto poly-L-lysine (0.01%; Sigma)) and laminin (10 μg/mL; Thermo Fisher) coated coverslips in 24-well plates, or directly on poly-L-lysine and laminin coated TC plates, in differentiation medium (Neurobasal, 2% B27, 1% NEAA, 1% Glutamax, 1% Penicillin/Streptomycin (all from Thermo Fisher)) lacking EGF and bFGF. After being allowed to attach and differentiate for 1–2 days, medium was replaced with fresh medium containing either 1 μg/mL AgNP (40 nm in citrate; Sigma) or 100 μM sodium citrate vehicle control. Stock solutions of LiCl (Thermo Fisher) in PBS1 or IWP4 (Tocris, Minneapolis, MN) in DMSO were added to final concentrations as specified in each experiment; control cells were treated with vehicle only (PBS1 or DMSO).

Differentiation of SVZ-NSC involves collection of suspended neurospheres of various sizes and densities, these are seeded in differentiation medium in the well plate where they settle to the bottom. Individual cells, responding to growth factor withdrawal and the laminin coating, attach to the substrate, migrate away, and extend dynamic neurites while differentiating. Each cell line derives from a cell culture obtained from an individual brain and represents a heterogeneous population. Due to the qualitative nature of the plating process, and because different cell lines are not consistent in how much individual cells migrate, the densities of resulting differentiating cultures can vary. Experiments were only analyzed if cell densities were within an acceptable range – sufficiently dense to find cells in randomly selected fields of view while sparse enough to provide plenty of migration space for individual cells.

B35 neuroblastoma cells were purchased from ATCC (Manassas, VA) and maintained in undifferentiated form as adherent culture in TC flasks in complete medium containing FBS (DMEM, 1% P/S, 10% FBS). Cells were passaged by trypsinization before reaching confluence. For experimentation, cells were trypsinized (Thermo Fisher) and plated in 6-well TC plates in medium lacking FBS to promote neural differentiation. AgNPs or citrate (control) was included in the medium as detailed for every experiment.

All cells were cultured at 37 °C and 5% CO_2. Stock AgNP suspension (40 nm; 0.02 mg/ml) in citrate buffer was commercially obtained (Sigma). As suggested by the manufacturer, stock solutions were re-tested within 6 months of opening to ensure that nanoparticle size and zeta potential remained consistent. Analysis was performed on the purchased AgNP suspension, diluted in citrate buffer (control), by dynamic light scattering (DLS) in-house (Brookhaven Instrument Corporation, Long Island, NY). A Zeta Potential Analyzer was employed to determine the direction of particles under the influence of an electric field, allowing for the estimation of the zeta potentials of the nanoparticles. All stock solutions contained AgNP with mean sizes of 40.7–53.7 (± 2.1) nm and zeta potentials of -6.78 to -43.3 (± 2.91) mV. Stock particles were analyzed only in citrate buffer, and protein corona formation or composition was not investigated. However, AgNP solutions in cell culture medium were made fresh as a universal stock for every experiment, aliquoted for addition of pharmacological agents, and immediately added to cells to ensure that all conditions were exposed to AgNP with equivalent surface modifications.

2.2. Comet assay

Because high concentrations of AgNPs are known to be cytotoxic, we used alkaline comet assay (Singh et al., 1988) to assess DNA damage in SVZ-NSC exposed to AgNPs at the low concentrations used in this study. Solutions were prepared in advance and stored at 4 °C. Cells were plated in differentiation medium in 6-well plates as described above. Following 2–3 days of attachment and differentiation, medium was replaced with differentiation medium (positive and negative controls) or medium containing 1 μg/mL or 2 μg/mL AgNPs. Flamed slides were dipped in molten 1% normal melt agarose (10 mg/mL in water), stored flat at 25 °C overnight, and warmed to 37 °C before use. Cells were lifted by scraping and collected by centrifugation. Resulting pellets were suspended in 500 μL either PBS1 (negative control and AgNP-treated) or 200 μM H_2O_2 in PBS1 (positive control only) and left on ice for 20 min. Cells were once again collected by centrifugation and re-suspended in 20 μL PBS1 at 37 °C. 10 μL of this suspension was mixed with 90 μL of molten low-melt agarose (LMA; 0.6 mg/mL in PBS1, final 0.55 mg/mL) at 37 °C and gently spread over pre-warmed slides. Slides were placed on an ice block at 4 °C for at least 30 min, until the LMA layer had solidified, before being immersed in lysis buffer at 4 °C (0.1 M EDTA (Sigma); 2.5 M NaCl (Fisher); 0.2 M NaOH (AMRESCO); 10 mM Tris (AMRESCO); 1% Triton-X; pH 10) in the dark for 1 h. Slides were moved to electrophoresis buffer (0.3 M NaOH; 1 mM EDTA; pH 13) in the dark for 1 h to allow for DNA denaturation. Slides were moved to fresh electrophoresis buffer in a horizontal gel apparatus and run at 1 V/cm and 300 mA for 30 min. Slides were then immersed in neutralization buffer (0.4 M Tris, pH 7.5) at room temperature four times 5 min, before being washed in diH_2O two times 5 min. Finally, slides were dehydrated in 70% ethanol for 5 min and allowed to dry at 37 °C for 15 min. Each slide was covered with 60 μL of 1 μg/mL DAPI to stain DNA, coverslipped, and imaged after 30 min using an epifluorescent microscope. Images were collected from an area of 10 × 10 fields of view from the center of each slide to form a mosaic image, with at least

50 cells per sample. Images were analyzed in Image J (NIH, Bethesda, MD) with the OpenComet plugin (Gyori et al., 2014).

DNA damage for individual cells is determined by measuring DNA mobility in electrophoresis where large nuclear DNA molecules form a 'head', and small DNA fragments migrate away to form a comet 'tail'. The OpenComet software quantifies DNA in the head and tail, calculating an Olive tail moment that represents the degree of DNA fragmentation. Small Olive moments are representative of intact DNA, while larger Olive moments indicate increased fragmentation (Olive and Banath, 2006).

2.3. Immunocytochemistry

In order to examine f-actin cytoskeleton morphology and expression patterns of β-catenin, we performed fluorescent labeling with phalloidin and immunocytochemistry on cells differentiated as above. Cells were washed with PBS1, fixed on coverslips with 4% paraformaldehyde for 15 min, washed with phosphate buffered saline 2 (PBS2; 100 mM sodium phosphate, 150 mM NaCl, pH 7.4) and then permeabilized with 0.3% Triton-X/PBS2 for 10 min. Preparations were blocked with 5% bovine serum albumin (BSA, Fisher) and 10% normal goat serum (NGS, Thermo Fisher) for 1 h before being incubated overnight with mouse α-β-catenin (Thermo Fisher) in block solution. Control preparations containing no primary antibody were included in each experiment. After 6-5 min washes with PBS2, preparations were incubated in goat-α-mouse Alexa 488 (Thermo Fisher) and phalloidin-Alexa 568 (Thermo Fisher) overnight in 5% BSA and 1% NGS solution. For some experiments, the antibodies were omitted and cells were stained only with phalloidin 568 for 20 min. All preparations were washed with PBS2 followed by counterstaining with DAPI. Coverslips were washed with diH_2O before being mounted on slides using Prolong Gold (Thermo Fisher). Slides were allowed to cure at room temperature overnight and stored at 4 °C. Images were acquired using epifluorescent microscopy. Cells were counted and staining intensity was measured in Image J (NIH, Bethesda, MD). Neurite lengths were determined using WIS-Neuromath software (Rishal et al., 2013), followed by manual sorting to ensure accurate cell identification and tracing.

2.4. Immunoblot

Immunoblot analysis was used on whole cell lysates from differentiating SVZ-NSC and cellular fractions from differentiating B35 cells to quantify levels of β-catenin protein in AgNP-exposed cells compared to control.

SVZ-NSC were differentiated overnight in 6-well plates as described above. Differentiation medium was replaced with fresh medium containing citrate control or AgNPs, and incubated overnight. Cells were washed twice with PBS1 and collected in SDS loading buffer (Cell Signaling Technologies, Danvers, MA) by scraping. Samples were sonicated for 15 s and heated to 95 °C for 10 min, then chilled on ice and stored at −20 °C.

B35 cells were differentiated for 2 days in 6-well TC plates as described above with citrate (control) or 1 μg/mL AgNP. Cells were washed with PBS1, lifted by trypsinization, and collected by centrifugation. Cellular compartments were fractionated to generate protein samples using a Kit (Cell Signaling Technologies) as per the manufacturer's instructions.

Samples were loaded in triplicate and protein was separated by electrophoresis on TGX Stain-Free acrylamide gels (Bio-Rad, Hercules, CA) and transferred to PVDF (GE, Piscataway, NJ). Images of total protein content were collected before and after transfer (ChemiDoc XRS + Imaging System, BioRad). Blots were blocked with 10% skim milk powder in Tween-Tris buffered saline (TTBS; 20 mM Tris, 500 mM NaCl, pH 7.5 plus 0.1% Tween20) for at least 1 h, washed with TTBS, and incubated overnight with mouse α-β-catenin in 5% bovine serum albumin (BSA) in TTBS at 4 °C. Blots were washed 5 x 5 min in TTBS and incubated with goat α-mouse-HRP (Cell Signaling) in BSA/TTBS for 1 h, washed again 5 x 5 min and developed with chemiluminescent detection reagent (Advansta, San Jose, CA). Images were collected from the chemiluminescent signal and at visible wavelengths (for molecular weight markers). Each band intensity was normalized to total protein in that lane (Image Lab Software, BioRad), the average of the triplicate lanes was calculated and then normalized to control levels for each sample.

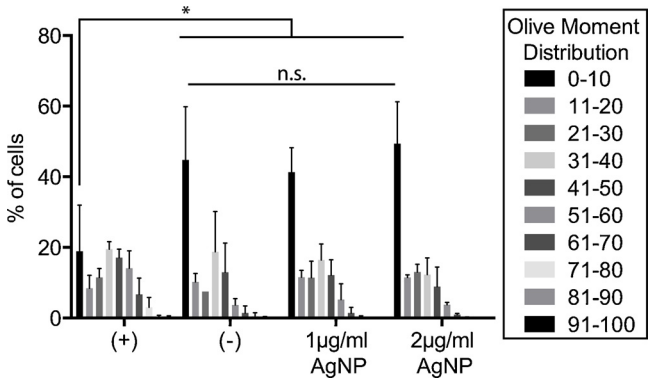

Fig. 1. SVZ-derived differentiating NSC do not experience genotoxicity from low-level AgNP exposure.
In positive control SVZ-NSC treated with H_2O_2 the proportion of cells exhibiting Olive moments of 0–10, indicative of little to no DNA damage, is reduced with a corresponding increase in the proportion of cells with high Olive moments indicating extensive DNA fractionation. In cells exposed to 1–2 μg/ml AgNPs for 24 h, however, the proportion of cells with low Olive moments is unchanged compared to negative control. (mean + SD, $p < 0.05$ ANOVA; *$p < 0.0001$, Sidak's multiple comparisons; 908-1607 cells per condition across 3 independent experiments).

2.5. Time lapse

Previously, we had found that AgNPs disrupted neurite dynamics in freely behaving differentiating SVZ-NSCs. We therefore used time lapse microscopy in combination with β-catenin pharmacology to examine the role of this signaling pathway in AgNP-mediated disruption of neurite dynamics. Neurospheres were plated for differentiation, as described above, on poly-L-lysine and laminin-coated chambered coverslips (Thermo Fisher) in differentiation medium made with neurobasal without phenol red. Cells were allowed to differentiate for 2 days. Half the medium was removed and replaced to achieve final concentrations of AgNPs and/or Li or IWP-4 as detailed for each experiment. Control wells received citrate and PBS1 or DMSO respectively. The chambered coverslip was immediately moved to a stagetop incubator on an inverted microscope (Leica, Buffalo Grove, IL). Transmitted light images from two fields of view in each well were collected every 30 min for 6 h. Neurite lengths were measured using the NeuronJ extension in ImageJ (Meijering et al., 2004).

2.6. Data analysis

Prism (Graphpad, San Diego, CA) was used for statistical analysis and generation of all graphs. Data in bar graphs are presented as mean + standard deviation as detailed. Statistics were performed as detailed for each experiment.

3. Results

3.1. Low-level AgNPs do not cause significant DNA damage in differentiating SVZ-NSC

The proportion of cells with significant DNA damage was assessed

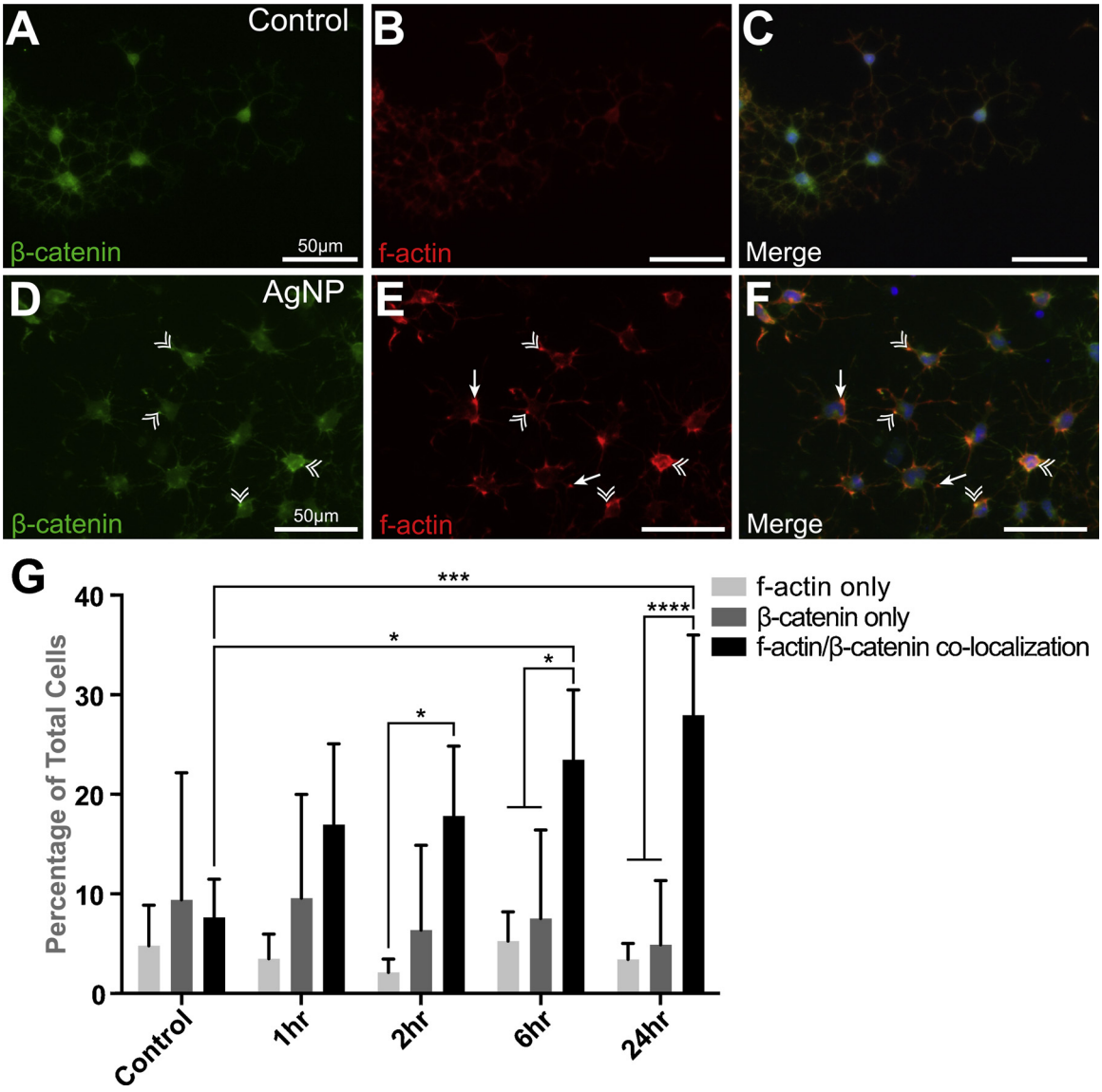

Fig. 2. Colocalized β-catenin aggregates and f-actin inclusions form in differentiating SVZ-NSC after AgNP exposure. A-C: Control SVZ-NSC do not form f-actin inclusions or β-catenin aggregates. **D-F:** 1 μg/mL AgNPs induce the formation of f-actin inclusions (D) and β-catenin aggregates (E). When overlaid (F), aggregates and inclusions (arrows) often co-localize (double arrowhead). **G:** The proportion of cells containing co-localized f-actin/β-catenin aggregates increases significantly over time, and is significantly different from those that contain only f-actin inclusions or β-catenin aggregates after AgNPs (mean + SD, $p = 0.0047$, Two-way ANOVA, $n = 6$ independent experiments using 4 different cell lines; *$p < 0.05$, ***$p < 0.001$, ****$p < 0.0001$; Sidak's multiple comparisons). Blue is DAPI. Scale bars are 50 μm. (For interpretation of the references to colour in this figure legend, the reader is referred to the web version of this article).

using the comet assay (Olive and Banath, 2006). In differentiating SVZ-NSC cells exposed to H_2O_2 to induce DNA damage as a positive control, a large proportion of cells exhibit high Olive moments, indicative of extensive fractionation of DNA. Conversely, the majority of cells in negative control, and after 24 h AgNPs (1 or 2 μg/mL), have Olive moments of 0-10. The proportion of cells with no significant DNA damage (Olive Moment 0–10) does not change significantly when comparing cells exposed to AgNPs to negative control (Fig. 1). This indicates that AgNPs at low levels up to 2 μg/mL do not induce DNA damage.

3.2. β-catenin co-localizes to f-actin inclusions in differentiating SVZ-NSC following low-level AgNP exposure

Immunocytochemistry was used to label β-catenin and f-actin within differentiating SVZ-NSC cells. As reported previously (Cooper and Spitzer, 2015), control cells had a relatively uniform distribution of f-actin, while low-level AgNP exposure (1 μg/mL; 24 h) induced the formation of f-actin inclusions (Fig. 2B, E). Similarly, β-catenin was uniformly distributed in control cells but formed aggregates in low-level AgNPs (Fig. 2A,D). Furthermore, the majority of β-catenin aggregates co-localized with f-actin inclusions (Fig. 2D–F, double arrowheads). The proportion of cells containing co-localized f-actin/β-catenin aggregates increased in a time-dependent manner during AgNP exposure (Fig. 2G). While a small proportion of cells contained f-actin inclusions or β-catenin aggregates only, these proportions did not change over time (Fig. 2G). These data indicate that protein aggregates that form in response to AgNP exposure contain both f-actin and β-catenin.

3.3. Low-level AgNPs modestly reduce intracellular β-catenin levels in SVZ-NSC

Differentiating SVZ-NSC were exposed to 1 μg/mL AgNPs for 24 h

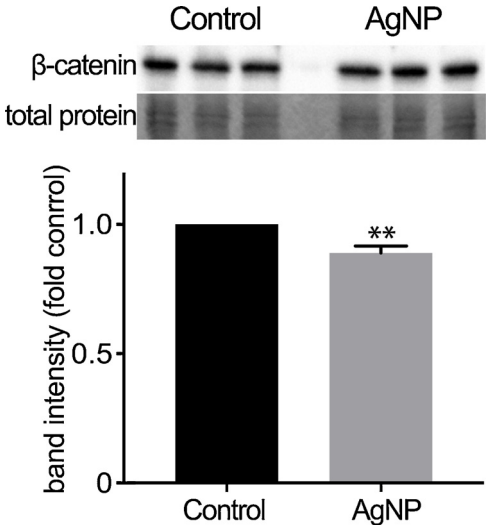

Fig. 3. β-catenin protein in differentiating SVZ-NSC is slightly reduced after low-level AgNP exposure. Intensity of β-catenin immunoblot bands was normalized to total protein in each lane. Mean intensity of β-catenin from cells exposed to 1 μg/ml AgNP for 24 h was reduced compared to control. Mean + SD, **p < 0.01, unpaired t-test. Each sample was run in triplicate in 3 independent experiments with 3 different cell lines.

before whole-cell homogenates were collected for immunoblot analysis. Total β-catenin in cells decreased by a small but significant amount following low-level AgNP exposure (Fig. 3). In β-catenin signaling, control is exerted through changes in intracellular levels of β-catenin itself (Wisniewska, 2013). Therefore, these results suggest a change in β-catenin signaling following AgNP exposure.

3.4. Low-level AgNPs do not alter intracellular β-catenin localization in differentiating SVZ-NSC or B35 cells

Because β-catenin signaling involves changes in the proportion of this protein in different cellular compartments, we investigated alterations in β-catenin distribution in differentiating SVZ-NSC after AgNP exposure. First, we used images of differentiated SVZ-NSC cells immunostained for β-catenin and analyzed the intensity of the signal across the soma. For each cell, a straight line was drawn across the soma, through the center of the nucleus. This provided intensity measurements for the edges (membranes) and cytoplasm of each soma. (Fig. 4A). Care was taken to avoid neurite extensions. Intensity values along lines were set to 0–100% of cell diameter, and normalized to the mean maximum intensity of control cells (Fig. 4B). The mean intensity of the β-catenin signal was significantly reduced in cells exposed to 1 μg/mL AgNPs for 24 h compared to control (Fig. 4B). This effect was reversed by the addition of 20 mM lithium (as LiCl), a β-catenin activator that acts by blocking glycogen synthase kinase 3β (GSK3β) (Panacek et al., 2006), thereby inhibiting β-catenin degradation.

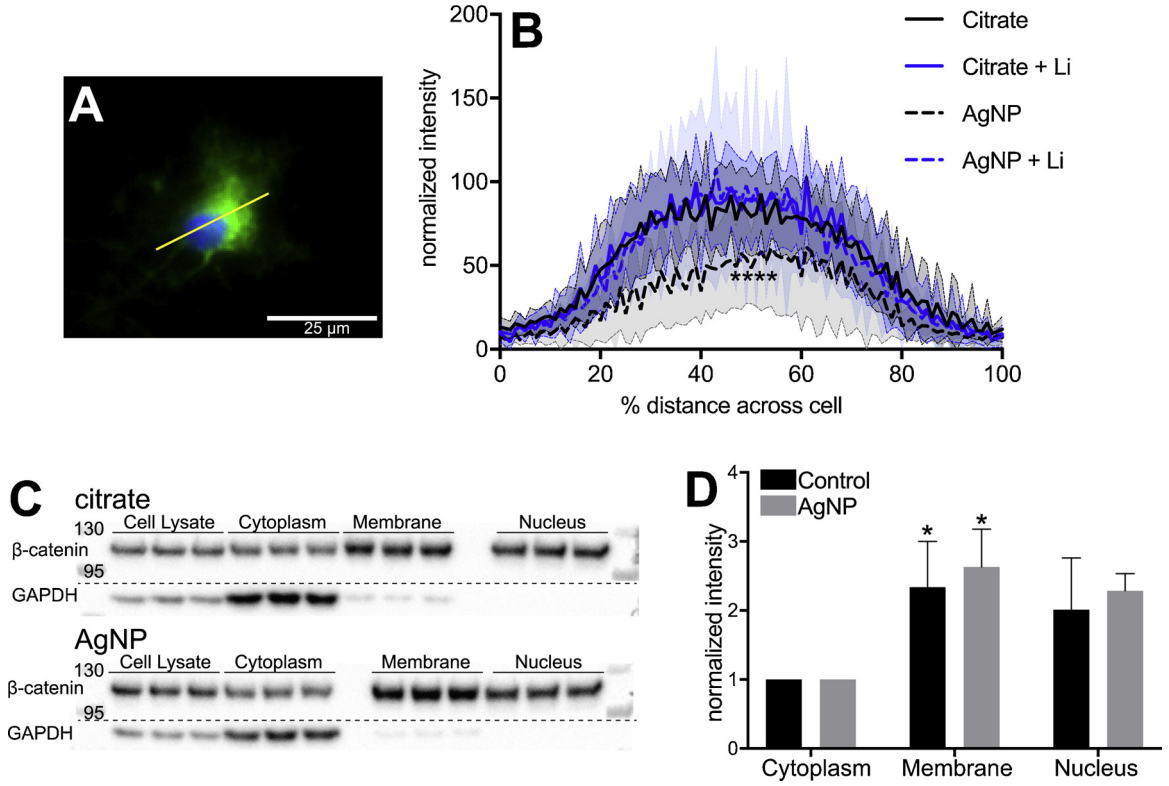

Fig. 4. Subcellular distribution of β-catenin in differentiating SVZ-NSC and B35 cells is not altered by AgNP exposure. A: Differentiating SVZ-NSC were immunostained for β-catenin (green) with DAPI counterstain (blue). Using ImageJ, a straight line was drawn across the center of the soma to generate a histogram of β-catenin label intensity for each pixel along the line. **B:** Values were normalized to distance across the cell and the mean maximum intensity in control cells (citrate only) was set to 100% for each experiment. Signal was evenly distributed across the soma in all conditions, and mean intensity was reduced in cells exposed to 1 μg/mL AgNPs compared to all other conditions (lines show mean intensity with SD illustrated by shaded regions, p < 0.0001 ANOVA, ****p < 0.0001 Tukey's multiple comparisons, 9–15 cells per condition in 3 independent experiments using 3 different cell lines). **C:** Immunoblot analysis of β-catenin (tops) in cell fractions of differentiating B35 neuroblastoma cells; each sample was run in triplicate. GAPDH immunoblot was performed (bottoms) to confirm fractionation of cellular compartments. **D:** β-catenin band intensity was normalized to stain-free total protein intensity in every lane and β-catenin in the cytoplasmic fraction was set to equal 1. No significant differences in relative β-catenin distribution was observed in AgNP exposed cells compared to control (mean + SD, p < 0.01 two-way ANOVA, *p < 0.05 compared to cytoplasm, Sidak's multiple comparisons). (For interpretation of the references to colour in this figure legend, the reader is referred to the web version of this article).

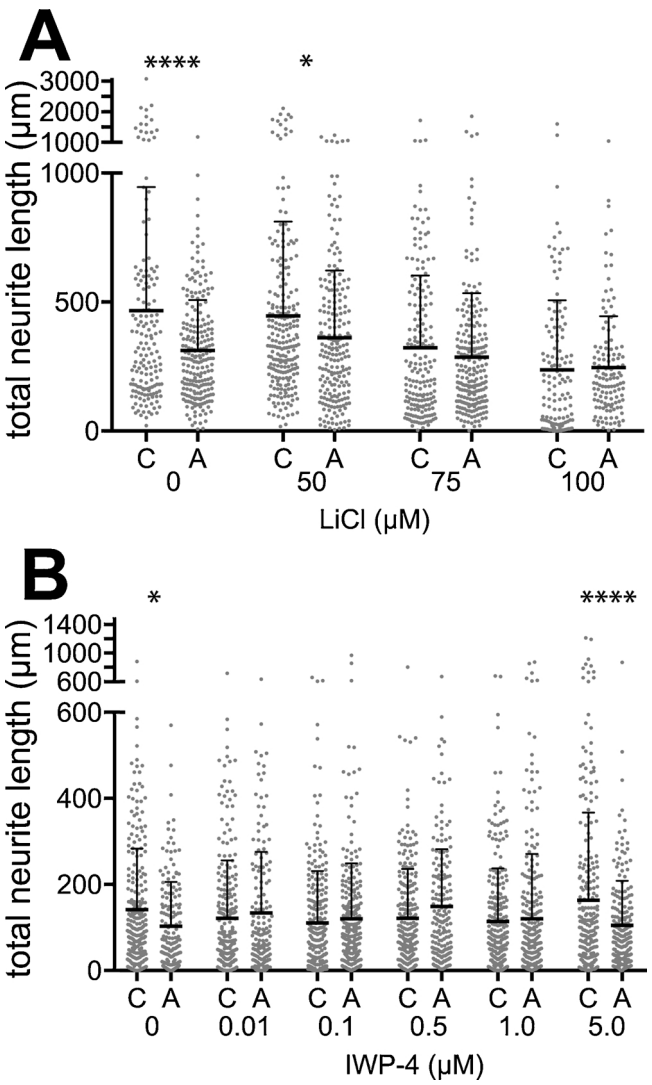

Fig. 5. Total neurite length of differentiating SVZ-NSC is reduced by AgNPs and modulated by β-catenin signaling, but β-catenin inhibition cannot counter AgNP effects. A: Differentiating SVZ-NSC have reduced total neurite length when exposed to AgNPs alone. The addition of the β-catenin signaling activator, lithium, elicits a dose-dependent reduction of total neurite length comparable to that observed in AgNPs. Neurite length reduction due to AgNP is not exacerbated by β-catenin activation with lithium. Dots represent individual cells in 6 independent experiments using 5 different cell lines, mean + SD are also shown. **B:** Pharmacological inhibition of β-catenin signaling with IWP-4 leads to increased total neurite length, but cannot counteract the reduction elicited by AgNPs exposure. "C": control; "A": AgNP. Dots represent individual cells in 8 independent experiments using 7 different cell lines, mean + SD are also shown. ($p < 0.01$ two-way ANOVA, *$p < 0.05$, ****$p < 0.0001$ AgNP vs. control, Sidak's multiple comparisons).

Interestingly, lithium treatment did not alter the mean β-catenin intensity or distribution in control cells. We did not observe intensity peaks near the periphery of the soma (0 and 100% distance across cell) that would indicate localization of β-catenin to the membrane of the soma.

Differentiating SVZ-NSC cells bind tightly to poly-lysine/laminin coated substrates and grow in low density; because of this we were not able to collect sufficient protein to perform cellular fractionation analysis. We therefore used differentiated B35 neuroblastoma cells to investigate changes in intracellular distribution of β-catenin after AgNP exposure via immunoblot. We previously demonstrated that B35 cells, like SVZ-NSCs, respond to low-level AgNPs with f-actin inclusions and neurite collapse (Cooper and Spitzer, 2015). Differentiating B35 cells were cultured, exposed to 24 h citrate control or 1 μg/mL AgNPs, and fractionated to generate protein samples. Samples were separated in triplicate by SDS-PAGE and analyzed by immunoblot for β-catenin with normalization to total protein (not shown) in each lane as described above (Fig. 4C, top band; D). We probed independently for the cytoplasmic protein GAPDH to confirm fractionation of cellular compartments (Fig. 4C, bottom band). The relative distribution of β-catenin in different cell fractions did not change in B35 cells following exposure to AgNPs (Fig. 4D).

3.5. AgNP and β-catenin signaling interact in regulating neurite growth in differentiating SVZ-NSC

Total neurite length (TNL) of SVZ-NSCs after 24 h exposure to AgNPs and/or a β-catenin activator or inhibitor was quantified using Neuromath software. SVZ-NSCs exposed to 1 μg/mL AgNPs alone for 24 h exhibited significantly reduced TNL compared to control (Fig. 5A, B). Activation of β-catenin signaling with lithium also resulted in a dose-dependent decrease of mean TNL. However, no significant difference was seen between TNL of control and AgNP-exposed cells for 75 and 100 μM LiCl (Fig. 5A). Therefore, AgNP alone, lithium alone, and AgNP plus lithium together resulted in comparable disruption of neurite extension.

To inhibit the β-catenin pathway, SVZ-NSCs were treated with IWP-4, a Wnt-specific inhibitor (Adachi et al., 2007), alone or with AgNPs. At lower concentrations of IWP-4, TNL of control and AgNP treated cells was highly variable, suggesting complex interactions of IWP-4 and AgNP. However, in 5 μM IWP-4, control cells showed significantly increased TNL while IWP-4 at this concentration was not able to overcome the reduction of TNL in cells exposed to AgNPs (Fig. 5B). Opposing effects of β-catenin signaling on TNL can be observed when comparing the highest concentrations used for activator and inhibitor of the pathway in the absence of AgNPs (Fig. 5A,B).

3.6. Modulation of β-catenin signaling interferes with AgNP-mediated formation of actin inclusions by differentiating SVZ-NSCs

Previously we reported that differentiating SVZ-NSC form actin inclusions in a dose-dependent response to low-level AgNP (Cooper and Spitzer, 2015) and that these inclusions co-localize with β-catenin aggregates (Fig. 2). We therefore treated differentiating SVZ-NSC with a β-catenin activator or inhibitor alone or in combination with 1 μg/mL AgNPs to assess formation of f-actin inclusions. As expected, there was a significant increase in the proportion of cells with f-actin inclusions after 24 h exposure to AgNPs compared to citrate control. Activation of β-catenin signaling with 100 μM lithium alone did not induce formation of f-actin inclusions. Furthermore, when cells were exposed to lithium and AgNP in combination, activation of β-catenin signaling appeared to counteract the formation of inclusions induced by AgNP alone (Fig. 6A). Interestingly, a similar interaction was observed between AgNPs and the β-catenin signaling inhibitor, IWP-4. The inhibitor alone (5 μM) did not alter inclusion formation, but interfered with AgNP-induced formation of f-actin inclusions (Fig. 6B). These data suggest that positive or negative manipulation of the β-catenin signaling pathway may interact with, and disrupt, the mechanism leading to f-actin inclusions in AgNP-exposed cells.

3.7. Disruption of neurite dynamics induced by AgNPs in differentiating SVZ-NSC cannot be rescued by modulating β-catenin signaling

Time-lapse microscopy of differentiating SVZ-NSC starting immediately after AgNP treatment allows investigation of neurite dynamics in individual identified cells that are freely behaving (Fig. 7A–D). Over six hours, the neurites of control cells actively extended and retracted, resulting in a variable but relatively constant

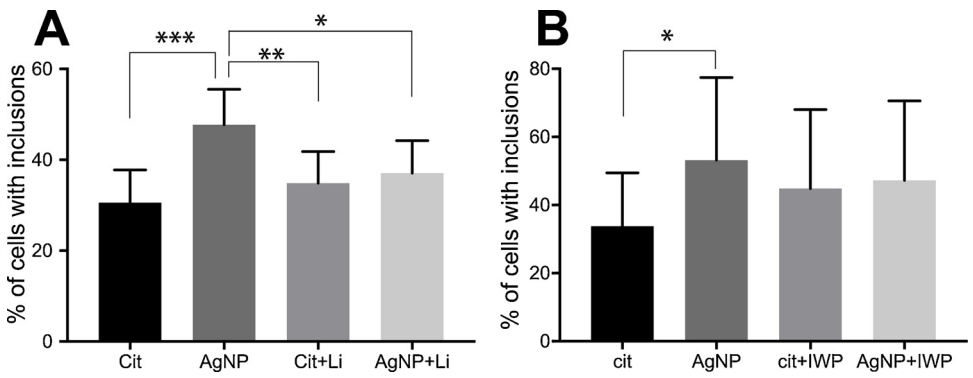

Fig. 6. AgNP-induced inclusion formation in differentiating SVZ-NSC is disrupted by pharmacological manipulation of β-catenin signaling. A: A larger proportion of SVZ-NSC exposed to 1 μg/ml AgNPs for 24 h form f-actin inclusions compared to citrate control. The addition of 100 μM lithium to activate β-catenin signaling had no effect on inclusion formation in control cells, but reduced the formation of inclusions in response to AgNPs. (mean + SD, $p < 0.001$, ANOVA. $^{**}p < 0.01$, Tukey's multiple comparisons. Mean of 9–108 cells per condition in 9 independent experiments using 8 different cell lines). **B.** Inhibition of Wnt/β-catenin signaling with 5 μM IWP-4 did not change inclusion formation and reduced f-actin inclusions formed in response to 24 h, 1 μg/ml AgNP exposure. (mean + SD, $p < 0.01$ repeated measures ANOVA, $^{*}p < 0.05$ Tukey's multiple comparisons, 7–156 cells per condition in 7 independent experiments using 6 different cell lines).

length. However, 1 μg/mL AgNP exposure resulted in collapse of individual neurite length and reduced branching within 6 h of exposure (Cooper and Spitzer, 2015) (Fig. 7B, E). Treatment with only the β-catenin signaling activator, lithium (100 μM), also resulted in neurite collapse, though loss in neurite length was not as dramatic as in AgNPs (Fig. 7C, E). When the two were combined, lithium activation of β-catenin signaling did not reduce neurite extension further or faster compared to AgNPs alone (Fig. 7D, E). These finding suggest that if AgNPs are interfering with neurite extension by activating the β-catenin signaling pathway, this low-level exposure represents maximal activation that cannot be increased by the addition of lithium.

When the β-catenin signaling pathway was inhibited with 5 μM IWP-4, freely behaving differentiating SVZ-NSC cells exhibit increased neurite outgrowth over time (Fig. 8C, E). This pharmacological treatment was, however, not able to achieve even partial rescue of neurite collapse elicited by 1 μg/mL AgNPs (Fig. 8D, E). The β-catenin signaling pathway is therefore irreversibly activated by AgNPs, or AgNPs disrupt neurite extension by an alternate mechanism that cannot be compensated for by inhibition of Wnt-specific β-catenin signaling.

4. Discussion

AgNPs are increasingly incorporated in consumer products including plastics, textiles, and appliances which then shed low levels of AgNPs into the environment leading to consumer exposure via inhalation or ingestion that is not yet well understood. Due to the unique physical properties of the nanoparticles, they are able to bypass the blood brain barrier and accumulate in the brain. Although the exposure to AgNPs from any one interaction with a consumer product is low (Bidgoli et al., 2013; Cushen et al., 2014), chronic exposure to multiple products, in combination with bioaccumulation, can lead to persistent AgNP in the brain (Lee et al., 2013). AgNP exposure of 1–5 μg/ml is not toxic to cultured neural cells (Haase et al., 2012; Hadrup et al., 2012; Xu et al., 2013), but the sub-lethal physiological effects of AgNP on neural cells is not well understood. We show here that, indeed, 1–2 μg/mL AgNP does not result in DNA damage typical of apoptosis and necrosis in cultured SVZ-NSC, indicating low cytotoxicity at this exposure level. However, we have previously reported changes in physiological functions (Cooper and Spitzer, 2015) in response to this low-level exposure to AgNPs.

The role of β-catenin in SVZ-NSC proliferation and differentiation, and therefore in adult neurogenesis, is highly complex (Adachi et al., 2007; Toledo et al., 2008; Varela-Nallar and Inestrosa, 2013; Wisniewska, 2013). Indeed, β-catenin has been found to play opposing roles in control of differentiation and proliferation, subject to signal context (Marinaro et al., 2012). Therefore, controlled β-catenin signaling is vital to SVZ-NSC and neurogenesis. Previously, we found that low-level AgNPs induced the formation of f-actin inclusions and disrupted neurite dynamics and arborization (Cooper and Spitzer, 2015). In differentiating neurons, neurite outgrowth is controlled by several modulatory mechanisms, including β-catenin signaling (Lee et al., 2014; Tang et al., 2010; Yu and Malenka, 2003). Here, we found that β-catenin is partially rearranged to form aggregates following exposure to AgNPs, and that these puncta co-localize with the f-actin inclusions. The β-catenin signaling protein may therefore be interacting with f-actin during AgNP-mediated cytoskeletal disruption, or it may be becoming trapped in nonspecific aggregates.

In cellular control cascades, β-catenin signaling involves modulation of levels of this effector protein with increased levels being a classic indicator of β-catenin signaling activation (Wisniewska, 2013). Activation of this signaling pathway is usually accompanied by translocation of β-catenin to the nucleus (Panacek et al., 2006; Xiu et al., 2011), though β-catenin has been shown to move to other cellular compartments like the membrane for signaling (Panacek et al., 2006). After AgNP exposure, we found a modest reduction in overall β-catenin levels, indicating that AgNP may interfere with β-catenin signaling. When analyzing the subcellular localization of β-catenin in SVZ-NSC, we found a generalized reduction in β-catenin signal intensity across the soma of AgNP cells. The intensity of the membrane did not increase overall, however, this analysis did not consider the highly localized f-actin/β-catenin aggregates that form in response to AgNP exposure. It is likely that most of the observed reduction in mean intensity in the soma is a result of concentration of β-catenin in these aggregates. Interestingly, blocking β-catenin degradation by GSK3β with lithium alone made no difference to overall signal intensity, suggesting the activation of homeostatic compensatory mechanisms, but returned the signal levels to control in cells also exposed to AgNPs. Furthermore, the distribution of β-catenin in cytoplasmic, nuclear, and membrane compartments did not change in response to AgNP exposure in B35 neuroblastoma cells. Together, these data indicate that AgNP exposure results in relocalization of β-catenin to protein aggregates within the cell, but likely does not greatly interfere with synthesis of this signaling molecule or activate specific signaling pathways involving directed relocalization of β-catenin to specific subcellular compartments.

Early-stage differentiating SVZ-NSC cultured in neurospheres, such as those studied here, are a mixed population, including cells at varying stages of differentiation towards neural and glial fates (Reynolds and Weiss, 1992; Wachs et al., 2003). Automated population analysis of total neurite length therefore resulted in highly variable data that are best examined on an individual cell basis as AgNP and pharmacological treatments have differential effects on the various cell types. Using this approach, we found a reduction in total neurite length after 24 h exposure to AgNP, in line with our previous results (Cooper and Spitzer, 2015). Interestingly, this reduction was reproduced when β-catenin levels were increased by lithium treatment. Conversely, inhibition of canonical Wnt/β-catenin signaling with IWP-4 resulted in neurite extension. However, IWP-4 was not able to reverse the reduction in neurite length elicited by AgNPs, indicating that any interaction

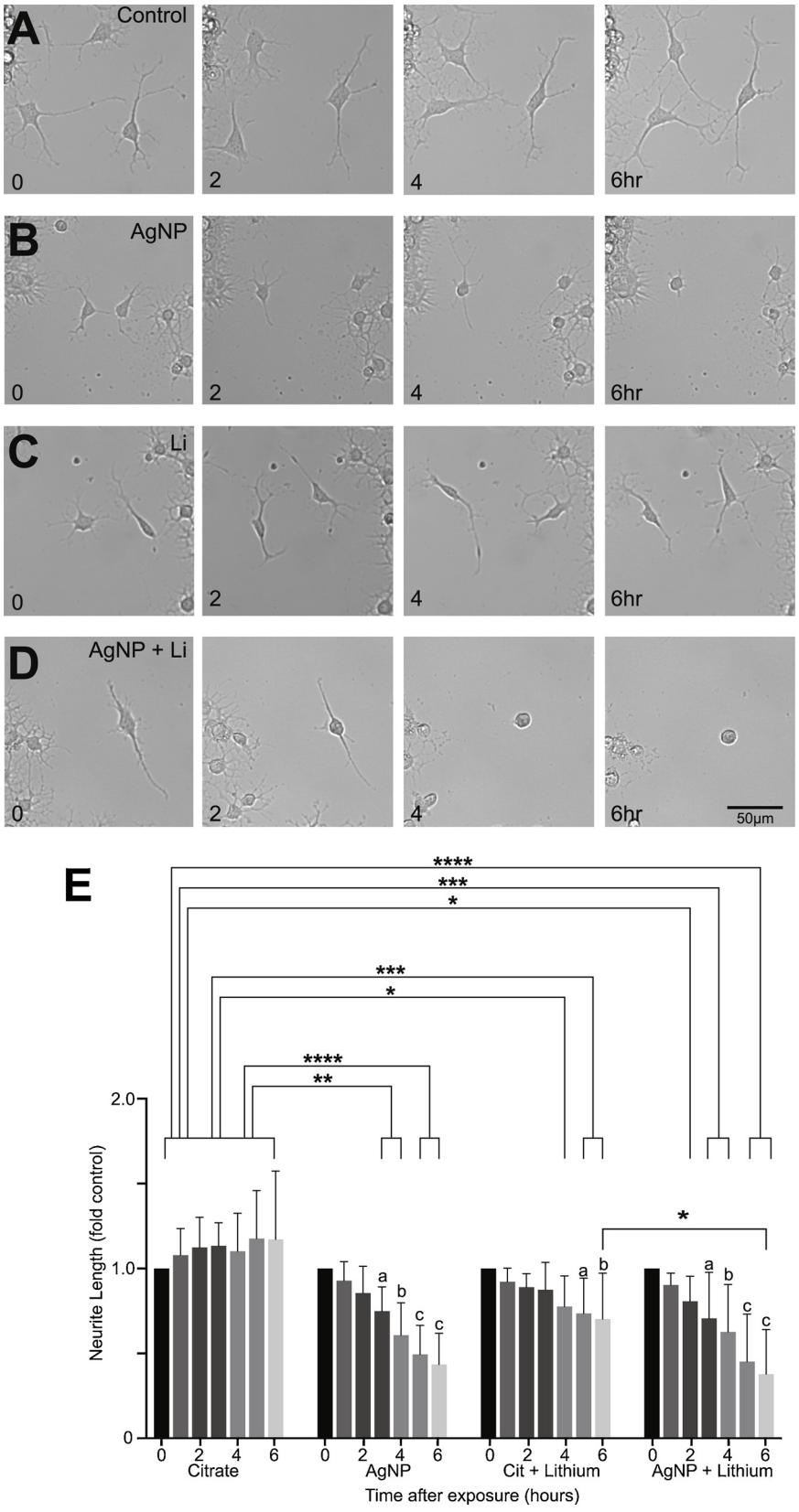

Fig. 7. Time lapse imaging of differentiating SVZ-NSC neurite dynamics in response to AgNP exposure and/or activation of β-catenin signaling. A-D: Control SVZ-NSC actively extend and retract neurites over a 6 h period. Cells suffer extensive collapse of neurites within 6 h of 1 μg/ml AgNP exposure, with or without activation of β-catenin signaling by lithium. **E:** The neurite collapse in response to AgNP exposure is rapid, leading to neurite lengths reduced by half within 6 h of exposure. The reduction in response to 100 μM lithium is not as rapid or severe. Combination of AgNPs with lithium results in neurite dynamics that are comparable to those observed in AgNPs alone. (mean + SD, $p < 0.05$, 2-way repeated measures ANOVA; $^{**}p < 0.01$, $^{***}p < 0.001$, $^{****}p < 0.0001$ compared to the same time point in citrate conditions. Lower-case letters indicate statistical differences between time points and control within experimental conditions. Sidak's multiple comparisons, 6 independent experiments with 2–6 cells per condition in every experiment).

between AgNP and the β-catenin signaling pathway may be non-canonical, indirect, or non-additive. Interestingly, both pharmacological activation and inhibition of β-catenin signaling resulted in a reduction in formation of f-actin inclusions in response to AgNPs. Exogenous manipulation of signaling may activate homeostatic mechanisms that help regulate cytoskeleton dynamics and structure, reducing inclusion formation, during the cellular response to AgNPs.

Due to the high variability and differential responses within the mixed population of SVZ-NSC cells, we used time lapse microscopy to study neuron-like cells individually as they responded to AgNPs in

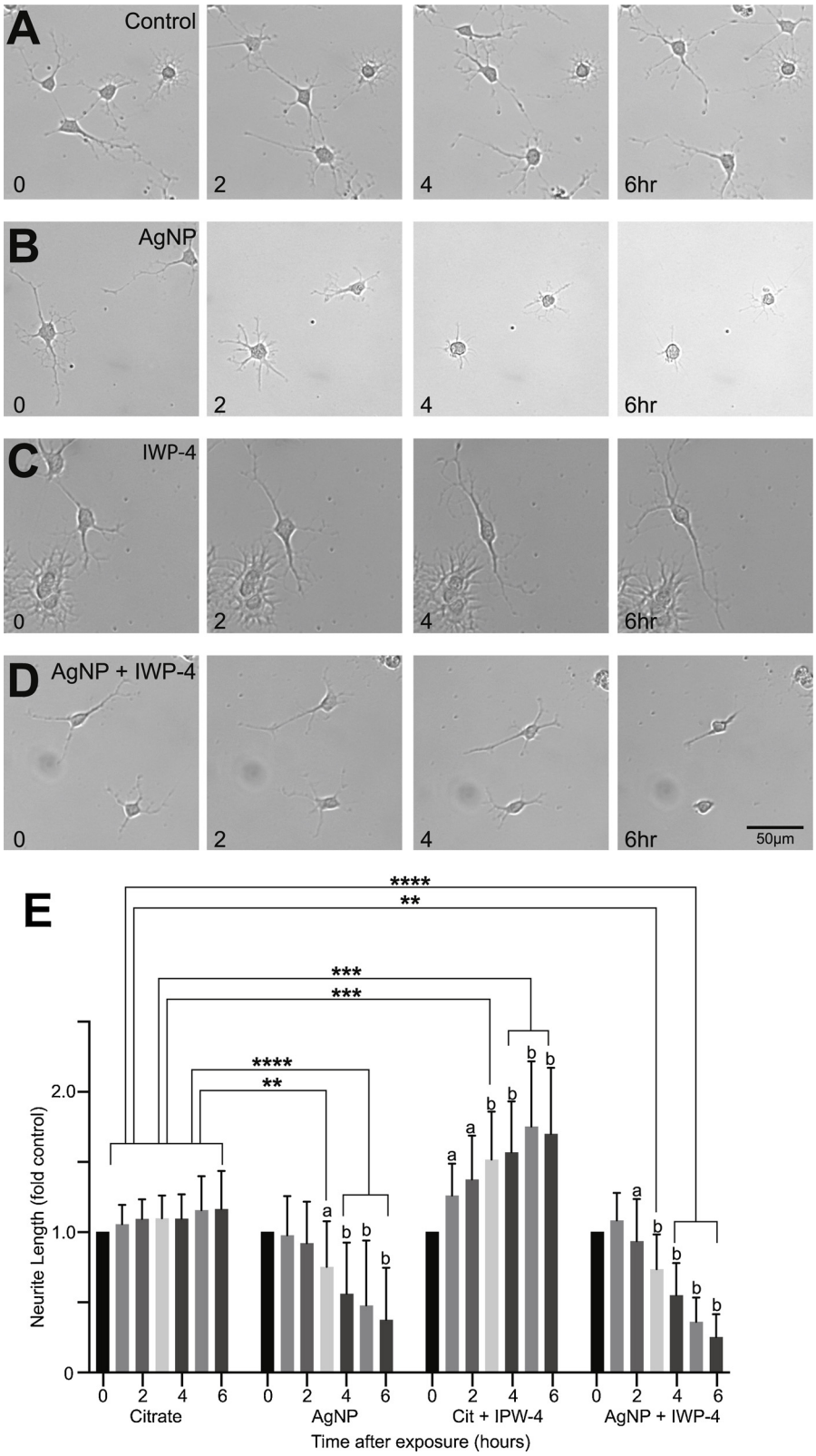

Fig. 8. Time lapse imaging of differentiating SVZ-NSC neurite dynamics in response to AgNP exposure and/or inhibition of β-catenin signaling. A-D: Control SVZ-NSC actively extend and retract neurites over a 6 h period. Cells suffer extensive collapse of neurites within 6 h of 1 µg/ml AgNP exposure. Inhibition of β-catenin signaling with 5 µM IWP-4 leads to extensive neurite outgrowth. **E:** IWP-4 stimulation of neurite outgrowth is not able to counteract the rapid neurite collapse elicited by AgNP exposure. ($p < 0.0001$, 2-way repeated measures ANOVA; $^{**}p < 0.01$, $^{***}p < 0.001$, $^{****}p < 0.0001$ compared to the same time point in citrate conditions. Lower-case letters indicate statistical differences between time points and control within experimental conditions. Sidak's multiple comparisons, 4 independent experiments with 2–6 cells per condition in every experiment).

combination with β-catenin pharmacological manipulation. As previously reported (Cooper and Spitzer, 2015), low-level AgNP exposure results in neurite collapse within 6 h of exposure. Activation of β-catenin signaling with lithium alone had a similar effect on neurite length, but did not result in additional reduction of neurite length in cells also exposed to AgNPs. Inhibition of β-catenin signaling with IWP-4 resulted in neurite extension that could not, however, overcome the collapse elicited by AgNPs.

Taken together, these results suggest that β-catenin signaling is being disrupted by low-level AgNP exposure, albeit in an indirect or non-additive manner. Previously, we showed that low-level AgNPs induce formation of f-actin inclusions and neurite collapse (Cooper and Spitzer, 2015). The data presented here indicate that β-catenin, normally a bridge between cadherin and the f-actin cytoskeleton in

adherens junctions (Toledo et al., 2008), may be sequestered within these inclusions. Indeed, upregulation of E-cadherin has previously been reported to perform this same function (Essuman et al., 2018). This sequestration may position β-catenin to better activate its downstream effectors, as AgNP treatment mimics the effect of pharmacological activation of β-catenin signaling on neurite extension. However, because the effect of AgNPs on neurite extension is not simply reversed by the addition of a β-catenin signaling inhibitor and total cellular β-catenin levels are slightly reduced by AgNP exposure, the interaction between the two mechanisms may be indirect or irreversible. The reduction in AgNP-induced formation of f-actin inclusions in response to pharmacological activation and inhibition of β-catenin signaling supports the idea that the relationship between the two mechanisms is nonlinear or complex. Because β-catenin signaling is involved in multiple cellular mechanisms involved in homeostasis and differentiation during all life stages, AgNP interaction with β-catenin could lead to abnormal signaling in neural cells and disruption of nervous system development and function.

Transparency document

The Transparency document associated with this article can be found in the online version.

Acknowledgements

We thank Dr. Rosalynn Quiñones and Grayce Behnke of the Marshall University Chemistry Department for performing periodic DLS and zeta potential analysis of AgNP stock solutions.

This work was supported by National Science Foundation (1553667 to NS and EPS-1003907). RJC and MNMC received support from the NASA WV SPACE Grant Consortium. JV acknowledges a fellowship from the SURE program funded through the Research Challenge Fund administered by the West Virginia Higher Education Policy Commission, Division of Science and Research, Grant Number: DSR. 17.09.

References

Adachi, K., Mirzadeh, Z., Sakaguchi, M., Yamashita, T., Nikolcheva, T., Gotoh, Y., Peltz, G., Gong, L., Kawase, T., et al., 2007. Beta-catenin signaling promotes proliferation of progenitor cells in the adult mouse subventricular zone. Stem Cells 25, 2827–2836. https://doi.org/10.1634/stemcells.2007-0177.

Addo Ntim, S., Norris, S., Goodwin Jr, D.G., Breffke, J., Scott, K., Sung, L., Thomas, T.A., Noonan, G.O., 2018. Effects of consumer use practices on nanosilver release from commercially available food contact materials. Food Addit. Contam. Part A Chem. Anal. Control Exposure Risk Assess. 35, 2279–2290. https://doi.org/10.1080/19440049.2018.1529437.

Aimone, J.B., Li, Y., Lee, S.W., Clemenson, G.D., Deng, W., Gage, F.H., 2014. Regulation and function of adult neurogenesis: from genes to cognition. Physiol. Rev. 94, 991–1026. https://doi.org/10.1152/physrev.00004.2014.

Altman, J., Das, G.D., 1965. Autoradiographic and histological evidence of postnatal hippocampal neurogenesis in rats. J. Comp. Neurol. 124, 319–335.

Bartlomiejczyk, T., Lankoff, A., Kruszewski, M., Szumiel, I., 2013. Silver nanoparticles – allies or adversaries? Ann. Agric. Environ. Med. AAEM 20, 48–54.

Bidgoli, S.A., Mahdavi, M., Rezayat, S.M., Korani, M., Amani, A., Ziarati, P., 2013. Toxicity assessment of nanosilver wound dressing in Wistar rat. Acta Med. Iran. 51, 203–208.

Cooper, R.J., Spitzer, N., 2015. Silver nanoparticles at sublethal concentrations disrupt cytoskeleton and neurite dynamics in culutted adult neural stem cells. Neurotoxicology 48, 231–238.

Cushen, M., Kerry, J., Morris, M., Cruz-Romero, M., Cummins, E., 2014. Evaluation and simulation of silver and copper nanoparticle migration from polyethylene nanocomposites to food and an associated exposure assessment. J. Agric. Food Chem. 62, 1403–1411. https://doi.org/10.1021/jf404038y.

Doetsch, F., Petreanu, L., Caille, I., Garcia-Verdugo, J.M., Alvarez-Buylla, A., 2002. EGF converts transit-amplifying neurogenic precursors in the adult brain into multipotent stem cells. Neuron. 36, 1021–1034. https://doi.org/10.1016/S0896-6273(02)01133-9.

Echegoyen, Y., Nerin, C., 2013. Nanoparticle release from nano-silver antimicrobial food containers. Food Chem. Toxicol. 62, 16–22. https://doi.org/10.1016/j.fct.2013.08.014.

Eriksson, P.S., Perfilieva, E., Bjork-Eriksson, T., Alborn, A.M., Nordborg, C., Peterson, D.A., Gage, F.H., 1998. Neurogenesis in the adult human hippocampus. Nat. Med. 4, 1313–1317. https://doi.org/10.1038/3305.

Essuman, V.A., Braimah, I.Z., Ndanu, T.A., Ntim-Amponsah, C.T., 2018. Presentation of children with advanced retinoblastoma for treatment in Ghana: the caretakers' perspectives. West Afr. J. Med. 35, 9–14.

Gage, F.H., 2000. Mammalian neural stem cells. Science 287, 1433–1438 DOI: 8300 [pii].

Garcia-Reyero, N., Kennedy, A.J., Escalon, B.L., Habib, T., Laird, J.G., Rawat, A., Wiseman, S., Hecker, M., Denslow, N., et al., 2014. Differential effects and potential adverse outcomes of ionic silver and silver nanoparticles in vivo and in vitro. Environ. Sci. Technol. 48, 4546–4555. https://doi.org/10.1021/es4042258.

Ge, S., Sailor, K.A., Ming, G.L., Song, H., 2008. Synaptic integration and plasticity of new neurons in the adult hippocampus. J. Physiol. 586, 3759–3765. https://doi.org/10.1113/jphysiol.2008.155655.

Gyori, B.M., Venkatachalam, G., Thiagarajan, P.S., Hsu, D., Clement, M.V., 2014. OpenComet: an automated tool for comet assay image analysis. Redox Biol. 2, 457–465. https://doi.org/10.1016/j.redox.2013.12.020.

Haase, A., Rott, S., Mantion, A., Graf, P., Plendl, J., Thunemann, A.F., Meier, W.P., Taubert, A., Luch, A., et al., 2012. Effects of silver nanoparticles on primary mixed neural cell cultures: uptake, oxidative stress and acute calcium responses. Toxicol. Sci. 126, 457–468. https://doi.org/10.1093/toxsci/kfs003.

Hadrup, N., Loeschner, K., Mortensen, A., Sharma, A.K., Qvortrup, K., Larsen, E.H., Lam, H.R., 2012. The similar neurotoxic effects of nanoparticulate and ionic silver in vivo and in vitro. Neurotoxicology 33, 416–423. https://doi.org/10.1016/j.neuro.2012.04.008.

Ivask, A., Elbadawy, A., Kaweeteerawat, C., Boren, D., Fischer, H., Ji, Z., Chang, C.H., Liu, R., Tolaymat, T., et al., 2014. Toxicity mechanisms in Escherichia coli vary for silver nanoparticles and differ from ionic silver. ACS Nano 8, 374–386. https://doi.org/10.1021/nn4044047.

Jamieson, C., Sharma, M., Henderson, B.R., 2012. Wnt signaling from membrane to nucleus: beta-catenin caught in a loop. Int. J. Biochem. Cell Biol. 44, 847–850. https://doi.org/10.1016/j.biocel.2012.03.001.

Jokar, M., Pedersen, G.A., Loeschner, K., 2017. Six open questions about the migration of engineered nano-objects from polymer-based food-contact materials: a review. Food Addit. Contam. Part A Chem. Anal. Control Expo. Risk Assess. 34, 434–450. https://doi.org/10.1080/19440049.2016.1271462.

Kruszewski, M., Brzoska, K., Brunborg, G., Asare, N., Dobrzyńska, M., Dušinská, M., Fjellsbø, L.M., Georgantzopoulou, A., Gromadzka-Ostrowska, J., et al., 2011. Toxicity of silver nanomaterials in higher eukaryotes. In: James, C.F. (Ed.), Advances in Molecular Toxicology. Elsevier, pp. 179–218.

Lee, J.H., Kim, Y.S., Song, K.S., Ryu, H.R., Sung, J.H., Park, J.D., Park, H.M., Song, N.W., Shin, B.S., et al., 2013. Biopersistence of silver nanoparticles in tissues from Sprague-Dawley rats. Part. Fibre Toxicol. 10, 36. https://doi.org/10.1186/1743-8977-10-36.

Lee, S.H., Ko, H.M., Kwon, K.J., Lee, J., Han, S.H., Han, D.W., Cheong, J.H., Ryu, J.H., Shin, C.Y., 2014. tPA regulates neurite outgrowth by phosphorylation of LRP5/6 in neural progenitor cells. Mol. Neurobiol. 49, 199–215. https://doi.org/10.1007/s12035-013-8511-x.

Marinaro, C., Pannese, M., Weinandy, F., Sessa, A., Bergamaschi, A., Taketo, M.M., Broccoli, V., Comi, G., Gotz, M., et al., 2012. Wnt signaling has opposing roles in the developing and the adult brain that are modulated by Hipk1. Cereb. Cortex 22, 2415–2427. https://doi.org/10.1093/cercor/bhr320.

Meijering, E., Jacob, M., Sarria, J.C., Steiner, P., Hirling, H., Unser, M., 2004. Design and validation of a tool for neurite tracing and analysis in fluorescence microscopy images. Cytometry A 58, 167–176. https://doi.org/10.1002/cyto.a.20022.

Muraoka, K., Shingo, T., Yasuhara, T., Kameda, M., Yuen, W.J., Uozumi, T., Matsui, T., Miyoshi, Y., Date, I., 2008. Comparison of the therapeutic potential of adult and embryonic neural precursor cells in a rat model of Parkinson disease. J. Neurosurg. 108, 149–159. https://doi.org/10.3171/JNS/2008/108/01/0149.

Olive, P.L., Banath, J.P., 2006. The comet assay: a method to measure DNA damage in individual cells. Nat. Protoc. 1, 23–29. https://doi.org/10.1038/nprot.2006.5.

Panacek, A., Kvitek, L., Prucek, R., Kolar, M., Vecerova, R., Pizurova, N., Sharma, V.K., Nevecna, T., Zboril, R., 2006. Silver colloid nanoparticles: synthesis, characterization, and their antibacterial activity. J. Phys. Chem. B 110, 16248–16253. https://doi.org/10.1021/jp063826h.

Quadros, M.E., Pierson, R., Tulve, N.S., Willis, R., Rogers, K., Thomas, T.A., Marr, L.C., 2013. Release of silver from nanotechnology-based consumer products for children. Environ. Sci. Technol. 47, 8894–8901. https://doi.org/10.1021/es4015844.

Reynolds, B.A., Weiss, S., 1992. Generation of neurons and astrocytes from isolated cells of the adult mammalian central nervous system. Science 255, 1707–1710.

Rishal, I., Golani, O., Rajman, M., Costa, B., Ben-Yaakov, K., Schoenmann, Z., Yaron, A., Basri, R., Fainzilber, M., et al., 2013. WIS-NeuroMath enables versatile high throughput analyses of neuronal processes. Dev. Neurobiol. 73, 247–256. https://doi.org/10.1002/dneu.22061.

Samuel, U., Guggenbichler, J.P., 2004. Prevention of catheter-related infections: the potential of a new nano-silver impregnated catheter. Int. J. Antimicrob. Agents 23 (Suppl 1), S75–8. https://doi.org/10.1016/j.ijantimicag.2003.12.004.

Singh, N.P., McCoy, M.T., Tice, R.R., Schneider, E.L., 1988. A simple technique for quantitation of low levels of DNA damage in individual cells. Exp. Cell Res. 175, 184–191.

Snyder, J.S., Kee, N., Wojtowicz, J.M., 2001. Effects of adult neurogenesis on synaptic plasticity in the rat dentate gyrus. J. Neurophysiol. 85, 2423–2431.

Sondi, I., Salopek-Sondi, B., 2004. Silver nanoparticles as antimicrobial agent: a case study on E. coli as a model for gram-negative bacteria. J. Colloid Interface Sci. 275, 177–182. https://doi.org/10.1016/j.jcis.2004.02.012.

Tang, J., Xiong, L., Wang, J., Liu, L., Li, J., Wan, Z., Xi, T., 2008. Influence of silver nanoparticles on neurons and blood-brain barrier via subcutaneous injection in rats. Appl. Surf. Sci. 255, 502–504. https://doi.org/10.1016/j.apsusc.2008.06.058.

Tang, J., Xiong, L., Zhou, G., Wang, S., Wang, J., Liu, L., Li, J., Yuan, F., Lu, S., et al.,

2010. Silver nanoparticles crossing through and distribution in the blood-brain barrier in vitro. J. Nanosci. Nanotechnol. 10, 6313–6317.
Toledo, E.M., Colombres, M., Inestrosa, N.C., 2008. Wnt signaling in neuroprotection and stem cell differentiation. Prog. Neurobiol. 86, 281–296. https://doi.org/10.1016/j.pneurobio.2008.08.001.
van Praag, H., Christie, B.R., Sejnowski, T.J., Gage, F.H., 1999. Running enhances neurogenesis, learning, and long-term potentiation in mice. Proc. Natl. Acad. Sci. U. S. A. 96, 13427–13431. https://doi.org/10.1073/pnas.96.23.13427.
Varela-Nallar, L., Inestrosa, N.C., 2013. Wnt signaling in the regulation of adult hippocampal neurogenesis. Front. Cell. Neurosci. 7, 100. https://doi.org/10.3389/fncel.2013.00100.
von Goetz, N., Fabricius, L., Glaus, R., Weitbrecht, V., Gunther, D., Hungerbuhler, K., 2013. Migration of silver from commercial plastic food containers and implications for consumer exposure assessment. Food Addit. Contam. Part A Chem. Anal. Control Exposure Risk Assess. 30, 612–620. https://doi.org/10.1080/19440049.2012.762693.
Wachs, F.P., Couillard-Despres, S., Engelhardt, M., Wilhelm, D., Ploetz, S., Vroemen, M., Kaesbauer, J., Uyanik, G., Klucken, J., et al., 2003. High efficacy of clonal growth and expansion of adult neural stem cells. Lab. Invest. 83, 949–962.
Wisniewska, M.B., 2013. Physiological role of beta-catenin/TCF signaling in neurons of the adult brain. Neurochem. Res. 38, 1144–1155. https://doi.org/10.1007/s11064-013-0980-9.
Xiu, Z.M., Ma, J., Alvarez, P.J., 2011. Differential effect of common ligands and molecular oxygen on antimicrobial activity of silver nanoparticles versus silver ions. Environ. Sci. Technol. 45, 9003–9008. https://doi.org/10.1021/es201918f.
Xu, F., Piett, C., Farkas, S., Qazzaz, M., Syed, N.I., 2013. Silver nanoparticles (AgNPs) cause degeneration of cytoskeleton and disrupt synaptic machinery of cultured cortical neurons. Mol. Brain 6, 29. https://doi.org/10.1186/1756-6606-6-29.
Yu, X., Malenka, R.C., 2003. Beta-catenin is critical for dendritic morphogenesis. Nat. Neurosci. 6, 1169–1177. https://doi.org/10.1038/nn1132.